

Ammonium Ion Removal using Activated Zeolite and Chitosan

N N Safie¹, A Y Zahrim^{1*} and N Hilal^{2,3}

¹ Faculty of Engineering, Universiti Malaysia Sabah, Jalan UMS, 88400 Kota Kinabalu Centre

² Water Advanced Technologies and Environmental Research (CWATER), College of Engineering, Swansea University, Swansea SA2 8PP, UK

³ NYUAD Water Research Center, New York University Abu Dhabi, Abu Dhabi, UAE

* E-mail: zahrim@ums.edu.my

Abstract. Studies have previously been done on efficacies of chitosan and zeolite in ammonium ion (NH_4^+) removal. However, no study compares the adsorption performance of natural zeolite and activated natural zeolite with high and low molecular weight chitosan. Hence, this study investigates the potentials of natural zeolite (NZ), activated natural zeolite (ANZ), low molecular weight chitosan (LMWC) and high molecular weight chitosan (HMWC) in NH_4^+ removal. The characteristics of NZ, ANZ, LMWC, and HMWC such as functional groups, surface morphology, elemental composition, zeta potential and particle size were also investigated. The deposition of NH_4^+ on the surface of NZ and ANZ was confirmed with the absence of nitrogen by the adsorption spectrum of EDX and supported by the presence of an FTIR stretching band at $\sim 3500\text{-}3300\text{ cm}^{-1}$, as well as broader and less intense bands $\sim 1600\text{ cm}^{-1}$ after the adsorption for all the adsorbents. The particle size of LMWC, HMWC, NZ and ANZ were 98, 813, 22354 and 9826 nm, respectively. Meanwhile, after the activation process, the composition of O, Si, Al, Fe, Ca and Na were reduced. NH_4^+ batch adsorption was also studied. HMWC, NZ, and ANZ reached adsorption equilibrium at 15 h, meanwhile for LMWC, the equilibrium reached at $t = 20$ h. The adsorption capacity of LMWC, HMWC, NZ, and ANZ at an initial concentration of 50 mg/L were 0.769 mg/g, 0.331 mg/g, 2.162 mg/g and 2.937 mg/g respectively. ANZ had the highest adsorption capacity, which might be related to the reduction of cationic elements such as Fe, Ca and Na after the activation has increased the unbalanced negative charge within the crystal lattice of ANZ that can be neutralized by NH_4^+ hence led to higher adsorption. HMWC has the lowest adsorption capacity that may be due it is positively

1 charged at pH 7 which would favor the adsorption of negatively charged species instead of
2 positively charged species, NH_4^+ .

3 Keywords: Ammonia; nitrogen; adsorption; natural; zeolite; chitosan

4 **1. Introduction**

5 NH_4^+ has been the cause of nitrogen pollution in recent years, originating from municipal and
6 industrial effluent caused by human activities such as surface runoff from farmland and residential
7 areas. In turn this causes nutrient enrichment which lead to serious eutrophication in urban drainage,
8 wastewater, and groundwater sources. Water pollution is linked to 14, 000 deaths daily, which NH_4^+
9 toxic contaminants are a contributor to [1]. The hazard posed by consuming NH_4^+ has led to stringent
10 water quality standards; as nitrate in drinking water from surface water shall not exceed 10 mg/L,
11 nitrite levels in drinking water usually below 0.1 mg/L and the allowable concentration for treated
12 effluent is 5 mg/L [2–4]. This has led to the necessity to have a competent wastewater treatment in
13 which can remove NH_4^+ to below the allowable limit.

14 There are many wastewater treatment methods available. Biological processes, such as
15 conventional activated sludge treatment, anaerobic-anoxic-oxic, sequencing batch reactor, and
16 oxidation ditch are reported to be less efficient in nitrogen removal due to inability to meet the
17 stringent nutrients discharge standards, instability treatment effect and time consuming process [5].

18 Ammonia stripping, electrodialysis, bioelectrical treatment suffer from drawbacks such as regular
19 maintenance, higher capital and operating expenses and lack of technology access and experts [6]. On
20 top of that, adsorption has gained extensive attention in NH_4^+ removal due to its low-cost, high affinity
21 towards NH_4^+ , efficiency and simplicity of application as well as environmental friendliness [7–9].
22 Processes based on the use of natural, locally available adsorbents are considered to be more
23 accessible for developing countries, have lower investment cost and lower environmental impact [10].

24 Recently, natural zeolites have been upgraded to a commodity of great capabilities such as
25 being used for the removal of NH_4^+ from municipal, industrial or agricultural waste and drinking

1 water [11]. Natural zeolites consist of three-dimensional frameworks of aluminosilicates where
2 oxygen, aluminium, and silicon are covalently bonded in a tetrahedral structure. Each aluminium
3 (Al^{3+}) atom substitution for silicon (Si^{4+}) atom in the zeolite framework which will generate one
4 negative charge within the pores that will be balanced by positively charged ions (cations) such as
5 Na^+ , K^+ , Ca^{2+} , and Mg^{2+} on the external surface of natural zeolite with weak electrostatic bonds that
6 caused the ability to be exchanged with other cations in solutions such as NH_4^+ [12–14]. Although
7 natural zeolites are available in abundance, their relatively small adsorption capacities for NH_4^+ (10
8 mg/g or less) [9] and lower efficacy as compared to synthetic zeolite which is reported to have greater
9 adsorption capacity due to higher proportion of higher specific area, bigger total pore volume and
10 lower average pore size has led to modification of natural zeolite [15,16].

11 Natural zeolite, such as fly ash, Australian natural zeolite and Chinese natural zeolite, have been
12 previously investigated but low adsorption capacity was recorded [14,16–18]. Several pre-treatments
13 have been done on natural zeolite, activated natural zeolite and commercial zeolite including acid,
14 base, salt, and organic surfactant treatments, before being used in NH_4^+ removal [16,18–20]. Heat
15 treatment is known to be the best pre-treatment due to the morphological structure changes which do
16 not require any chemicals. The pore size decreases, but the content of cations will also greatly reduce,
17 opening up more sites for the attachment of NH_4^+ [18,21]. The temperature used during heat treatment
18 plays an important role. Heat treatment at 400 °C and lower have a positive impact as the adsorption
19 capacity will improve compared to non-treated natural zeolite. However, according to Zhang et al.
20 [22], who studied activation temperature of 500 °C to 700 °C, reported that high heat treatment
21 reduced the adsorption of $\text{NH}_3\text{-N}$ due to the degradation of an important element, O, changing the
22 isoelectric point.

23 Other than natural zeolite, chitosan, a non-toxic natural carbohydrate polymer derived from the
24 chitin component of crustacean exoskeletons such as shrimp, crab, crawfish, etc., was reported to be
25 an excellent adsorbent material because it contains hydroxyl (-OH) and amino (- NH_2) groups that
26 serve as binding sites [23]. The mechanism of adsorption of ion on the surface of chitosan was

1 explained by Zhang and Bai [24]. Chitosan has been used in heavy metals removal [25] and dye
2 adsorption [26].

3 Many studies have been done on chitosan and zeolite separately as suitable adsorbents for NH_4^+
4 but no study compares adsorption performance of natural zeolite, activated natural zeolite with high
5 and low molecular weight chitosan. For instance, Kołodyńska et al. [17] reported the comparison of
6 modified natural zeolite with different molecular weights of chitosan, but those were used to treat
7 methylene blue and copper, Cu (II) ion instead of NH_4^+ . Yang et al. [18] compared only one molecular
8 weight of chitosan with natural zeolite. Teimouri et al. [27] compared chitosan with commercial
9 zeolite instead of natural zeolite for nitrate ion (NO_3^-) removal. Haseena et al.[28] studied hybrid
10 commercial zeolites such as zeolite Y and bentonite clay with no modification but no comparison was
11 made with chitosan. Hence, this paper fills in these gaps by reporting studies of the capability of
12 natural adsorbents: natural zeolite, modified natural zeolite, low molecular weight chitosan and high
13 molecular weight chitosan whose characterizations and ammonium ion adsorption capacities were
14 investigated.

15 **2. Methodology**

16 *2.1. Materials*

17 The natural zeolite originated from Indonesia. The chemical composition of natural zeolite from
18 supplier was (SiO_2 : 65.5 %, Al_2O_3 : 12.5 %, Fe_2O_3 : 1.35 %, CaO : 2.6 %, MgO : 1.22 %, Na_2O : 0.63 %, K_2O : 1.6 %, TiO_2 : 0.01 % and cationic exchange capacity (CEC): 1.40 meq/g). LMWC (50,000 –
19 190,000 Da, 75-85% deacetylated) (Sigma Aldrich) and HMWC (310000 – 375000 Da, > 75 %
20 deacetylated) (Sigma Aldrich, USA). It was used directly without further purification. Nessler reagent
21 was used to analyze NH_4^+ which consisted of a Nessler reagent, mineral stabilizer and polyvinyl
22 alcohol dispersion, range of detection limit: 0.02 – 2.5 mg/L (Hach, USA).

24 *2.2. Preparation of adsorbents*

25 The natural zeolite was washed and dried at 104 °C overnight. The activated natural zeolite was
26 prepared by using the method by Taaca et al. [29]. Firstly, the natural zeolite was broken down into

1 fine powders using mortar and pestle before the treatment procedure. The particles were washed with
2 distilled water and filtered twice. The slurry was dried at 105° C for 2 h and active treatment followed
3 at 120 °C for 6 h. All solids were stored in a dry place to avoid moisture. Low molecular weight
4 chitosan, high molecular weight, natural zeolite, and activated natural zeolite were denoted as LMWC,
5 HMWC, NZ, and ANZ.

6 2.3. *Functional groups identification*

7 The functional groups present in LMWC, HMWC, natural zeolite and activated natural zeolite before
8 and after the adsorption were recorded by using Fourier transform infrared (FTIR) spectrometer
9 (Perkin Elmer Spectrum-100). The spectra were recorded in the wavenumber range from 4000 to 400
10 cm⁻¹.

11 2.4. *SEM-EDX*

12 The detailed surface morphology of LMWC, HMWC, NZ, and ANZ before use were obtained by
13 using a scanning electron microscope (SEM, S-3400 N, Hitachi) coupled with energy dispersive X-ray
14 (EDX) spectrometer with 10.0 kV acceleration voltage with a magnification range of 180 until 13 k.
15 The samples were coated with gold by a sputter coater Q150RS before analysis to increase the
16 conductivity of the samples. The approximation of pore size and the sizes of flakes were done for all
17 the adsorbents.

18 2.5. *Zeta potentials and particle size*

19 0.1 g NZ, ANZ, LMWC, and HMWC was suspended in 100 g of distilled water, followed by stirring
20 at 200 rpm for 24 h. Before the analysis, each sample was distributed into the vials. The pH values
21 were adjusted to 7 by addition of 0.1 M HCl or 0.1 M NaOH solution. Dynamic light scattering (DLS)
22 was used to measure the hydrodynamic diameter (diameter in nanometer range in (d.nm) and laser
23 Doppler anemometry (LDA) was used to measure the zeta potential in (mV) [30]. DLS and LDA were
24 performed using a Zetasizer Nano ZS instrument (Malvern Panalytical Ltd. UK).

25

1 *2.6. Batch adsorption*

2 Equilibrium tests were conducted to determine the equilibrium adsorption capacity for LMWC,
3 HMWC, NZ, and ANZ. For the reaction, 500 g of NH₄Cl solution with an initial concentration of 50
4 mg/L was poured inside a 1000 mL beaker. 5 g of NZ and ANZ were used. Meanwhile, 1 g of LMWC
5 and HMWC were used for the adsorption. pH was adjusted to 7 by the addition of 0.1 M NaOH or
6 0.1 M HCl stock solutions. The temperature was set to 30 °C (room temperature), with a stirring speed
7 of 700 rpm. 2.5 mL of solution was pipetted out for 30 min, 1 h, 2 h, 6 h, 12 h, and 24 h. Three
8 replicates were done per adsorbent type. The samples were then analysed using a Jasco UV-vis 650
9 Bio-spectroscopy with a maximum wavelength of 425 nm. Before analysis, Nessler reagent was used
10 for ammonia nitrogen compound detection by following the standard USEPA Nessler Method
11 No.8038. The concentration of ammonium ion adsorbed at equilibrium was calculated as in equation
12 (1).

13

$$q_e = \frac{(C_o - C_e)V}{W} \quad (1)$$

14 **3. Results and discussions**

15 *3.1. Characterizations of adsorbents*

16 *3.1.1. Functional groups identification*

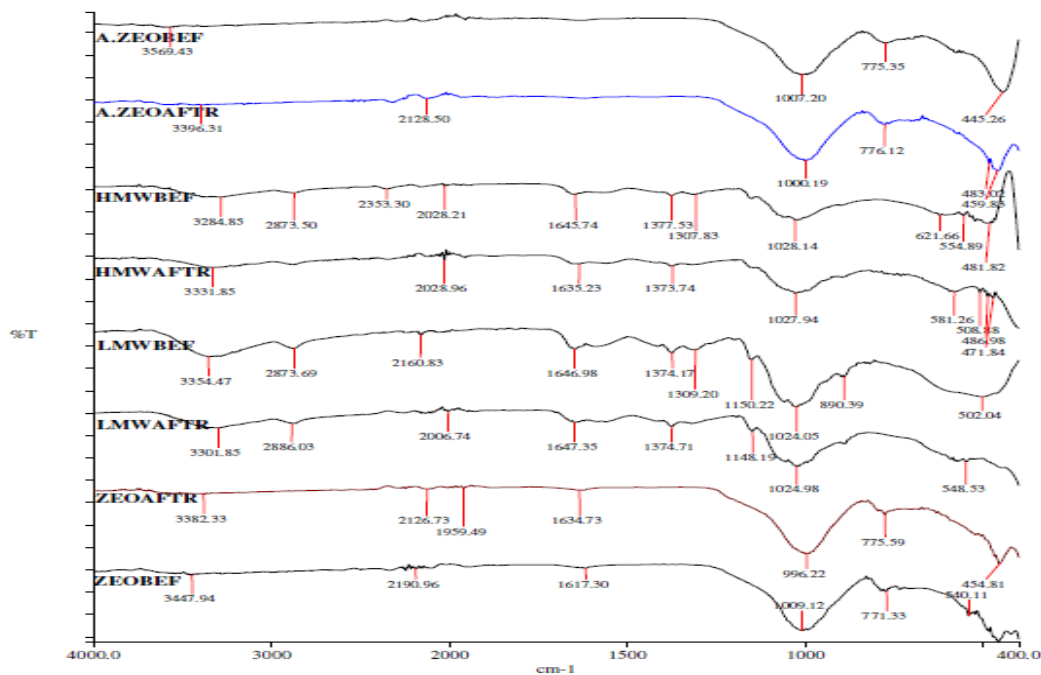
17 The FT-IR spectra for NZ, ANZ, LMWC and HMWC for before and after the adsorption reaction are
18 depicted in figure 1. All adsorbents showed stretching vibrations at ~3500-3300 cm⁻¹. Both O-H and
19 N-H stretch at wavenumbers above 3100 cm⁻¹, but O-H will show a more intense band than N-H
20 [27,31]. NZ, ANZ, LMWC, and HMWC had shown an intense peak at range ~3500-3300 cm⁻¹ but the
21 band showed medium and broad shape after the adsorption which indicated the presence of N-H bond.
22 This has confirmed the attachment of NH₄⁺ after the adsorption process.

23 Before the adsorption, HMWC and LMWC had shown stretching vibration with medium peak
24 intensity at 3300 – 2700 cm⁻¹ which is for the C-H compound [31,32]. This has been confirmed with

1 the formation of band at $\sim 1380\text{ cm}^{-1}$ which is the indication of methyl group. The compound has fewer
2 than four adjacent methylene groups because there is no absorption band at $\sim 720\text{ cm}^{-1}$.

3 There are bands at the range of $\sim 2260 - 2100\text{ cm}^{-1}$ shown by ANZ, HMWC, LMWC, NZ
4 before and after the adsorption which indicated for the presence of triple bond of C and triple bond of
5 C and N. N-H bending vibrations also occur at $\sim 1600\text{ cm}^{-1}$ and absorption at that wavelength does not
6 always indicate a C=C bond. However, absorption bands resulting from the N-H bend tend to be
7 broader (due to hydrogen bonding) and more intense due to being more polar) than those caused by
8 C=C stretches [31].

9



10

11

12

Figure 1. FTIR analysis.

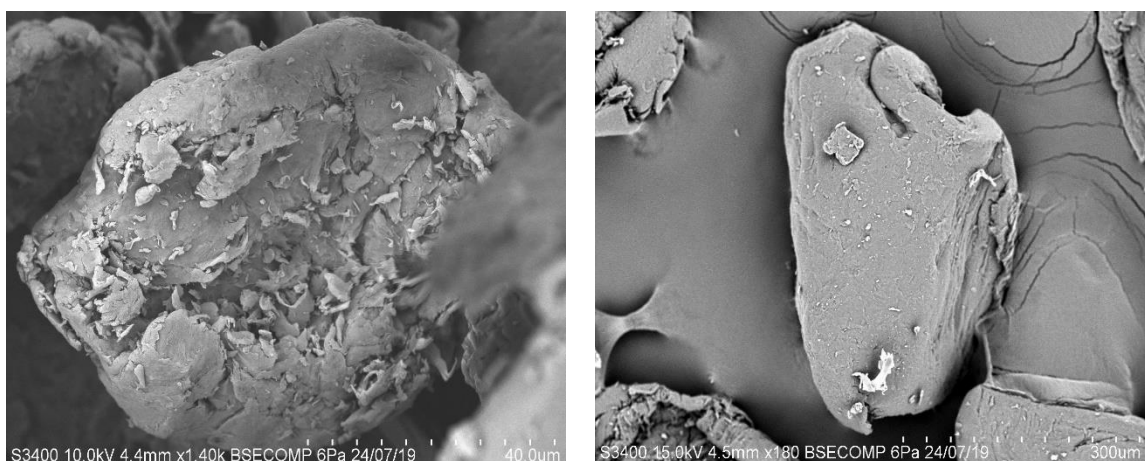
13 Band around $\sim 1000.14\text{ cm}^{-1}$ is a bending vibration of Si-O [33] and ~ 1018 stretching
14 vibrations of the Y zeolite structure framework [27] which have been shown by both NZ and ANZ.

1 The major peak at 1023 cm^{-1} and 1015 cm^{-1} justifies Si-O-Si asymmetric stretching and bending
2 respectively [34]. NZ and ANZ showed bands at $775.35\text{ cm}^{-1} - 776.12\text{ cm}^{-1}$ and $775.59\text{ cm}^{-1} - 771.33$
3 cm^{-1} were due to the quartz or amorphous SiO_2 stretching vibration and Si-O-Si bending mode [32].

4 *3.1.2. Morphological structure*

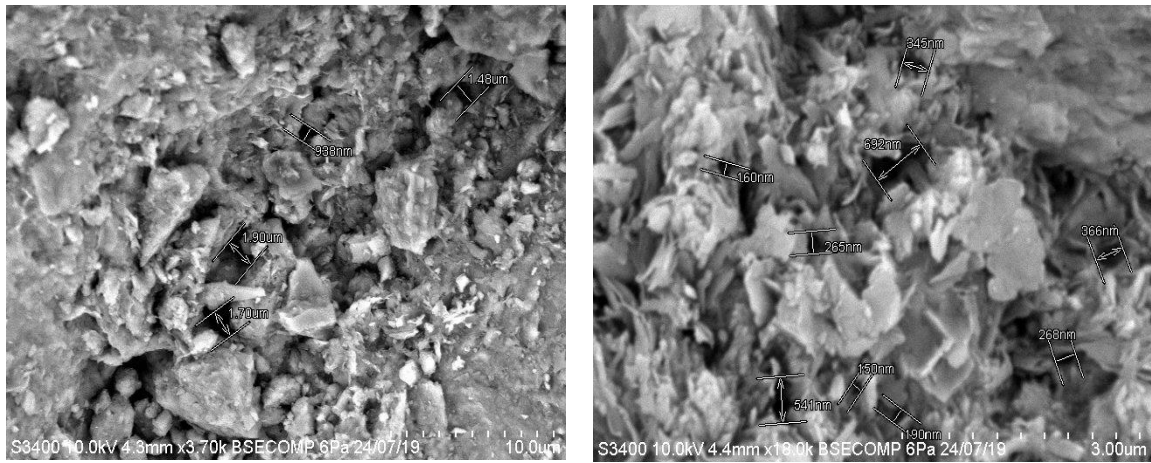
5 The surface morphological structures of LMWC, HMWC, NZ, and ANZ are depicted in figure 2 (a)-
6 (d). In SEM analysis, the surface morphology was taken at an acceleration voltage of 10kV and with
7 magnifications 180 until 13 k. From the results, rough surface was noticed for HMWC, LMWC, NZ,
8 and ANZ. As shown in figure 2 (a) and (b), an irregular shape of flakes like structure with no
9 distinctive pore was observed for both LMWC and HMWC. This was also being observed by Cui et
10 al.[35] in the commercial chitosan. Meanwhile, irregular pores for NZ and ANZ were noticed as
11 illustrated in figure 2 (c) and (d). Powder like structure was observed for NZ but not for ANZ, as the
12 structure changed to flakes like structure with more pores were observed. Furthermore, irregular
13 cracks have also being noticed on the ANZ surface in figure 2 (d). The estimated pore size of NZ and
14 ANZ was $1153.8\text{ }\mu\text{m}$ and $825.32\text{ }\mu\text{m}$ respectively. It was noted that the activation had caused the pore
15 size to decrease.

16



(a)

(b)



(c)

(d)

Figure 2. SEM analysis (a) LMWC, (b) HMWC, (c) NZ, (d) ANZ.

1

2 *3.1.3. Elemental Analysis*

3 As presented in Table 1, the elemental composition of LMWC, HMWC, NZ, and ANZ before the
 4 adsorption test were studied using the EDX. The elements of C, O, and N were detected for LMWC
 5 and HMWC. These elements are the common elements present in most chitosan due to the presence of
 6 free amine, carboxyl and hydroxyl groups that functions as active sites during the adsorption process
 7 [25].

8 The presence of the elements Si, Al, O, Na, Ca and Fe were detected due to the natural zeolites
 9 which are composed of three dimensional frameworks of aluminosilicate where the aluminium and
 10 silicon structure atoms are bound by covalent bond over shared oxygen atoms to form interconnected
 11 cages and channels. These will form pores and is where most of the cations are present and ion
 12 exchange processes occur [14,36]. It was noticed that after the activation, the composition of O, Si,
 13 and Al had decreased. The decrease of element O is suspected to be due to the loss of H₂O. The
 14 decrease of exchangeable cations such as Na, Ca, Fe by 12 %, 47 %, and 10 % respectively.

15

16

17

18

1

Table 1. EDX analysis.

Adsorbent	Element composition (wt. %)							
	C	O	N	Si	Al	Na	Ca	Fe
HMWC	53.250	21.223	9.215	-	-	-	-	-
LMWC	50.975	21.905	8.9075	-	-	-	-	-
NZ	1.548	41.130	0	34.278	9.130	0.603	3.513	3.933
ANZ	7.510	38.418	0	30.280	8.450	0.503	1.855	3.550

2 **3.1.4. Zeta Potentials**

3 The measured zeta potentials of NZ, ANZ, HMWC, and LMWC at pH 7 are shown in table 2. As can
4 be seen, LMCW, HMCW, NZ, and ANZ have zeta potentials of -46.8 mV, 6.4 mV, -36.7 mV and 34.9
5 mV respectively. The particle size of LMCW, HMWC, NZ and ANZ were 98, 813, 22354 and 9826
6 nm, respectively. The size of LMWC is smaller than HMWC. From Table 2, NZ has larger particle
7 size compared to ANZ. This has shown that the heat pretreatment has reduced the particle size of NZ.
8 The reduction of particle size has proven that the activation process has occurred.

9

Table 2. Zeta potentials and particle sizes

Adsorbent	Zeta Potentials (mV)	Particle size (nm)	
		(This study)	(Other study)
LMCW	-46.8	98.41 DD : 77 %, MW: 131 kDa	308.4[37] DD : 90.4 %, MW : 66.3 kDa
HMWC	6.4	813.57 DD : > 75 %, MW : 343 kDa	543.8[37] DD : 90.2 %, MW : 316 kDa
NZ	-36.7	22354	17660 [38]
ANZ	-34.9	9826	4580 [38]

10 **3.2. Ammonia nitrogen batch adsorption**

11 Figure 3 illustrates the concentration of NH_4^+ adsorbed on the surface of LMWC, HMWC, NZ, and
12 ANZ as a function of the contact time. HMWC, NZ, and ANZ reached adsorption equilibrium at 15 h,
13 whereas for LMWC, the equilibrium was reached at $t = 20$ h. LMWC required more time to reach
14 equilibrium which is due to its lower deacetylation degree (DD) which lowers its stability during the
15 reaction [39].

16

17

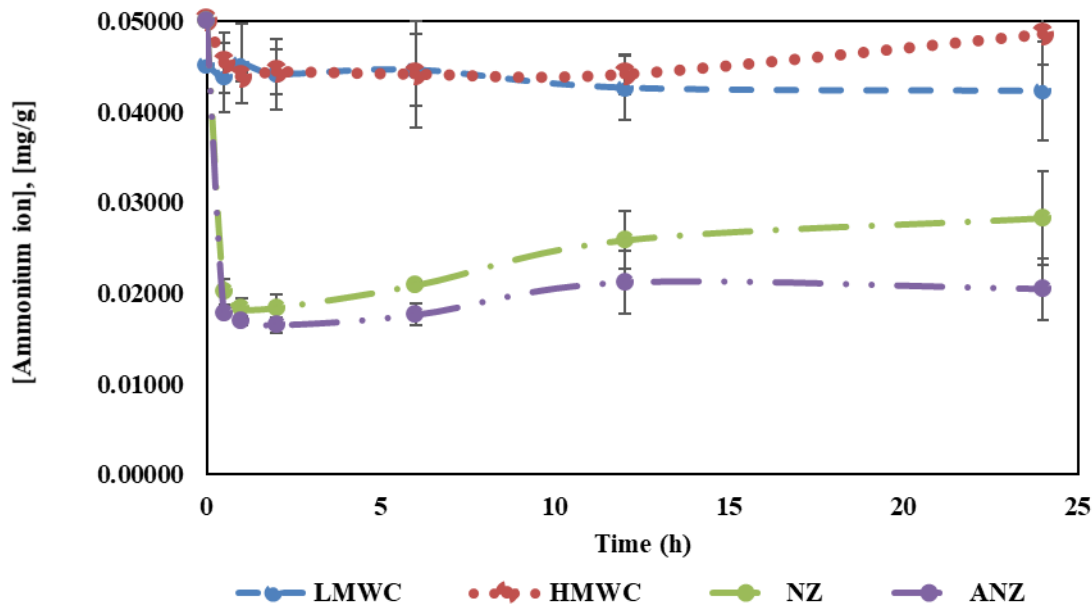


Figure 3. Adsorption of ammonium ion at different time intervals using LMWC, HMWC, NZ, and ANZ.

The adsorption capacity of LMWC, HMWC, NZ, and ANZ at an initial concentration of 50 mg/L were 0.769 mg/g, 0.331 mg/g, 2.162 mg/g and 2.937 mg/g respectively. ANZ had the highest adsorption capacity compared to LMWC, HMWC, and NZ. This was due to the decrement of cationic species Na, Ca and Fe which was detected by EDX analysis for ANZ, which contributed to the higher unbalanced negative charge within the crystal lattice of ANZ that can be neutralized by NH_4^+ hence led to higher adsorption [18,20,21]. This is also supported by the findings of Yang et al. [18] who reported that the activation using heat treatment caused the adsorption capacity of natural zeolite to improve due to the decrease of exchangeable cations. Furthermore, the reduction of particle size from 22354 nm to 9826 nm after the activation process has also contributed to higher sorbent performance because a fresh surface is exposed, and the total outer surface area is increased [38,40].

The effect of the molecular weight of chitosan and DD has been studied on the adsorption of NH_4^+ . In this study, HMWC with higher DD (>75 %) contains higher amino groups which were confirmed by EDX analysis which showed that it has higher nitrogen content compared to LMWC

1 (DD: 75-85 %). It was found that HMWC has a lower adsorption capacity compared to LMWC. Li et
2 al. [41] also observed that the adsorption capacity of chitosan with lower DD was higher compared to
3 chitosan that has high DD. The same finding has also been observed by Chung et al. [42] where low
4 molecular weight has higher removal for ammonia (NH₃) compound compared to high molecular
5 weight chitosan.

6 Based on the zeta potentials tabulated in Table 2, LMWC, NZ, and ANZ are negatively charged
7 at pH 7 that may enhance the adsorption of NH₄⁺, hence, higher adsorption capacity recorded except
8 for HMWC which is positively charged at pH 7. From the electrostatic interaction point of view, the
9 positive zeta potentials would favour the adsorption of negatively charged species instead of positively
10 charged species, NH₄⁺ which may lower the adsorption capacity [43]. Chitosan acts as a weak base at
11 lower value of DD and the cationicity as well as pKa of the chitosan will importantly increase at DD
12 over 80 % due to the presence of amino groups of glucosamine which responsible for cationic nature
13 and net positive charge of chitosan under acidic or neutral condition [44–46]. DD determines the
14 number of acetamide groups (C₂H₅NO) that randomly distributed along the C2 atoms along the
15 chitosan chain which will affect the conformational charge of chitosan when in a solution and
16 solubility. Furthermore, there is a possibility of hydrogen bonds (intra or intermolecular bonds) that
17 reduced the number of accessible free amines for the cations uptake [47].

18 The second factor that may attribute to the low adsorption capacity of HMWC is due to it has a
19 bigger particle size compared to LMWC as tabulated in Table 2. The particle sizes of HMWC and
20 LMWC are 813.57 nm and 98.41 nm respectively. In research reported by Guibal et al.[48], the
21 adsorption capacity was found to be lower, which was attributed to the larger particle size of the
22 flakes. The large particle size of HMWC will occupy large volume in the reactor that leads to less
23 mobility of adsorbents during the reaction, meanwhile, LMWC which is smaller in size has lesser
24 resistance towards flow and hence higher exposed surface area [49]. Even though LMWC is more
25 negative and has smallest particle size among NZ and ANZ, however, the reactions may be hindered
26 brought about by the number of acetyl groups and formation of hydrogen bond between the other

1 LMWC and water compounds as well as the effect of swelling may contribute to the low adsorption
2 capacity [50,51].

3 However, based on Figure 3, there is an increasing trend of adsorption at 24th h for all
4 adsorbents used in this study. The same trend was observed by Zahrim & Hilal [52] for dye removal,
5 Bernardi et al. [53] in removal of total ammonia using chitosan and Masheanne et al.[54] in nitrate
6 removal using chitosan. There is probability of desorption since this can perhaps be explained by the
7 fact that the process involves several mechanisms such as physico-chemical adsorption, ion-exchange,
8 precipitation or complexation as controlling step that can act simultaneously during batch adsorption
9 using chitosan [54–56].

10 **4. Conclusion**

11 This work shows the characterization and adsorption capacity of natural zeolite (NZ), activated natural
12 zeolite (ANZ), low molecular weight chitosan (LMW) and high molecular weight chitosan (HMWC).
13 Based on the FTIR and EDX analysis, it was confirmed there was attachment of NH_4^+ to the surface of
14 NZ, ANZ, LMW, and HMWC. The activation on natural zeolite had caused the pore size, particle size
15 as well as the composition of O, Si, Al, Fe, Ca and Na to be decreased. HMWC, NZ, and ANZ
16 reached adsorption equilibrium at 15 h, meanwhile for LMWC, the equilibrium reached at $t = 20\text{h}$.
17 The adsorption capacity of LMWC, HMWC, NZ and ANZ at initial concentration 50 mg/L were 0.769
18 mg/g, 0.331 mg/g, 2.162 mg/g and 2.937 mg/g respectively. ANZ employed the highest adsorption
19 capacity due to the vacant sites for ion exchange to occur after the activation process. Meanwhile,
20 HMWC recorded the lowest adsorption capacity because it is positively charged and as such favours
21 negatively charge ions instead of positively charged species, such as NH_4^+ .

22 **5. References**

- 23 [1] Zhang Y, Zheng F and Cao N 2010 Effect of Saturated Near Surface on Nitrate and Ammonia
24 Nitrogen Losses in Surface Runoff at the Loess Soil Hillslope *Int. J. Chem. Eng.* **2010** 1–7
- 25 [2] National Water Services Commission 2013 *Malaysian Sewerage Industry Guidelines* (Kuala
26 Lumpur, Malaysia)

- 1 [3] Azreen I, Lija Y and Zahrim A Y 2017 Ammonia nitrogen removal from aqueous solution by
2 local agricultural wastes *IOP Conf. Ser. Mater. Sci. Eng.* **206**
- 3 [4] Chen J, Wu H, Qian H and Gao Y 2017 Assessing Nitrate and Fluoride Contaminants in
4 Drinking Water and Their Health Risk of Rural Residents Living in a Semiarid Region of
5 Northwest China *Expo. Heal.* **9** 183–95
- 6 [5] Li K, Liu Q, Fang F, Luo R, Lu Q, Zhou W, Huo S, Cheng P, Liu J, Addy M, Chen P, Chen D
7 and Ruan R 2019 Microalgae-based wastewater treatment for nutrients recovery: a review
8 *Bioresour. Technol.* 121934
- 9 [6] Eskicioglu C, Galvagno G and Cimon C 2018 Approaches and processes for ammonia
10 removal from side-streams of municipal effluent treatment plants *Bioresour. Technol.* **268** 797–
11 810
- 12 [7] Yin H, Yang C, Jia Y, Chen H and Gu X 2018 Dual removal of phosphate and ammonium
13 from high concentrations of aquaculture wastewaters using an efficient two-stage infiltration
14 system *Sci. Total Environ.* **635** 936–46
- 15 [8] Yaser A Z and Safie N N 2020 Sewage Treatment in Campus for Recycling Purpose: A
16 Review *Green Engineering for Campus Sustainability* (Singapore: Springer Singapore) pp
17 207–43
- 18 [9] Huang J, Chow C, Teasdale P R, Kankanamge N R, Welsh D T and Li T 2018 Removing
19 ammonium from water and wastewater using cost-effective adsorbents: A review *J. Environ.*
20 *Sci. (China)* **63** 174–97
- 21 [10] Asere T G, Stevens C V. and Du Laing G 2019 Use of (modified) natural adsorbents for
22 arsenic remediation: A review *Sci. Total Environ.* **676** 706–20
- 23 [11] Chmielewska E 2019 Natural zeolite: Alternative adsorbent in purification or post-treatment of
24 waters *Modif. Clay Zeolite Nanocomposite Mater.* 87–112
- 25 [12] Rožić M, Cerjan-Stefanović Š, Kurajica S, Vančina V and Hodžić E 2000 Ammoniacal
26 nitrogen removal from water by treatment with clays and zeolites *Water Res.* **34** 3675–81
- 27 [13] Peters K E, Walters C C and Moldowan J M 2004 *The Biomarker Guide* (Cambridge:
28 Cambridge University Press)
- 29 [14] Widiastuti N, Wu H, Ang H M and Zhang D 2011 Removal of ammonium from greywater
30 using natural zeolite *Desalination* **277** 15–23
- 31 [15] Lin L, Lei Z, Wang L, Liu X, Zhang Y, Wan C, Lee D J and Tay J H 2013 Adsorption
32 mechanisms of high-levels of ammonium onto natural and NaCl-modified zeolites *Sep. Purif.*
33 *Technol.* **103** 15–20
- 34 [16] Alshameri A, Ibrahim A, Assabri A M, Lei X, Wang H and Yan C 2014 The investigation into
35 the ammonium removal performance of Yemeni natural zeolite: Modification, ion exchange
36 mechanism, and thermodynamics *Powder Technol.* **258** 20–31
- 37 [17] Kołodyńska D, Hałas P, Franus M and Hubicki Z 2017 Zeolite properties improvement by
38 chitosan modification—Sorption studies *J. Ind. Eng. Chem.* **52** 187–96

- 1 [18] Yang K, Zhang X, Chao C, Zhang B and Liu J 2014 In-situ preparation of NaA
2 zeolite/chitosan porous hybrid beads for removal of ammonium from aqueous solution
3 *Carbohydr. Polym.* **107** 103–9
- 4 [19] Arora M, Eddy N K, Mumford K A, Baba Y, Perera J M and Stevens G W 2010 Surface
5 modification of natural zeolite by chitosan and its use for nitrate removal in cold regions *Cold*
6 *Reg. Sci. Technol.* **62** 92–7
- 7 [20] Liu J, Cheng X, Zhang Y, Wang X, Zou Q and Fu L 2017 Zeolite modification for adsorptive
8 removal of nitrite from aqueous solutions *Microporous Mesoporous Mater.* **252** 179–87
- 9 [21] Wibowo E, Sutisna, Rokhmat M, Murniati R, Khairurrijal and Abdullah M 2017 Utilization of
10 Natural Zeolite as Sorbent Material for Seawater Desalination *Procedia Eng.* **170** 8–13
- 11 [22] Zhang W, Fu R, Wang L, Zhu J, Feng J and Yan W 2019 Rapid removal of ammonia nitrogen
12 in low-concentration from wastewater by amorphous sodium titanate nano-particles *Sci. Total*
13 *Environ.* **668** 815–24
- 14 [23] Ngah W S W and Fatinathan S 2008 Adsorption of Cu(II) ions in aqueous solution using
15 chitosan beads, chitosan–GLA beads and chitosan–alginate beads *Chem. Eng. J.* **143** 62–72
- 16 [24] Zhang X and Bai R 2003 Mechanisms and kinetics of humic acid adsorption onto chitosan-
17 coated granules *J. Colloid Interface Sci.* **264** 30–8
- 18 [25] Vakili M, Deng S, Cagnetta G, Wang W, Meng P, Liu D and Yu G 2019 Regeneration of
19 chitosan-based adsorbents used in heavy metal adsorption: A review *Sep. Purif. Technol.* **224**
20 373–87
- 21 [26] Pietrelli L, Francolini I and Piozzi A 2015 Dyes Adsorption from Aqueous Solutions by
22 Chitosan *Sep. Sci. Technol.* **50** 1101–7
- 23 [27] Teimouri A, Nasab S G, Vahdatpoor N, Habibollahi S, Salavati H and Chermahini A N 2016
24 Chitosan /Zeolite Y/Nano ZrO₂ nanocomposite as an adsorbent for the removal of nitrate from
25 the aqueous solution *Int. J. Biol. Macromol.* **93** 254–66
- 26 [28] Haseena P V, Padmavathy K S, Krishnan P R and Madhu G 2016 Adsorption of Ammonium
27 Nitrogen from Aqueous Systems Using Chitosan-Bentonite Film Composite *Procedia Technol.*
28 **24** 733–40
- 29 [29] Taaca K L M and Vasquez M R 2017 Fabrication of Ag-exchanged zeolite/chitosan
30 composites and effects of plasma treatment *Microporous Mesoporous Mater.* **241** 383–91
- 31 [30] Vandana M and Sahoo S K 2009 Optimization of physicochemical parameters influencing the
32 fabrication of protein-loaded chitosan nanoparticles *Nanomedicine* **4** 773–85
- 33 [31] Bruice P Y 2011 *Organic Chemistry* ed D Giovanniello and N Folchetti (United States,
34 America: Pearson)
- 35 [32] Dehghani M H, Dehghan A and Najafpoor A 2017 Removing Reactive Red 120 and 196 using
36 chitosan/zeolite composite from aqueous solutions: Kinetics, isotherms, and process
37 optimization *J. Ind. Eng. Chem.* **51** 185–95

- 1 [33] Zhu K, Fu H, Zhang J, Lv X, Tang J and Xu X 2012 Studies on removal of NH₄⁺-N from
2 aqueous solution by using the activated carbons derived from rice husk *Biomass and Bioenergy*
3 **43** 18–25
- 4 [34] Sharma A, Syed Z, Brighu U, Gupta A B and Ram C 2019 Adsorption of textile wastewater on
5 alkali-activated sand *J. Clean. Prod.* **220** 23–32
- 6 [35] Cui L, Gao S, Song X, Huang L, Dong H, Liu J, Chen F and Yu S 2018 Preparation and
7 characterization of chitosan membranes *RSC Adv.* **8** 28433–9
- 8 [36] Englert A H and Rubio J 2005 Characterization and environmental application of a Chilean
9 natural zeolite *Int. J. Miner. Process.* **75** 21–9
- 10 [37] Zhang W, Zhang J and Xia W 2012 The preparation of chitosan nanoparticles by wet media
11 milling *Int. J. Food Sci. Technol.* **47** 2266–72
- 12 [38] Wibowo E, Sutisna, Rokhmat M, Khairurrijal and Abdullah M 2016 Why does thermal shock
13 produce smaller particles of zeolite? *Powder Technol.* **301** 911–9
- 14 [39] Habiba U, Afifi A M, Salleh A and Ang B C 2017 Chitosan/(polyvinyl alcohol)/zeolite
15 electrospun composite nanofibrous membrane for adsorption of Cr⁶⁺, Fe³⁺ and Ni²⁺ *J.*
16 *Hazard. Mater.* **322** 182–94
- 17 [40] Saastamoinen J, Pikkarainen T, Tourunen A, Räsänen M and Jäntti T 2008 Model of
18 fragmentation of limestone particles during thermal shock and calcination in fluidised beds
19 *Powder Technol.* **187** 244–51
- 20 [41] Li F and Ding C 2011 Adsorption of reactive black M-2R on different deacetylation degree
21 chitosan *J. Eng. Fiber. Fabr.* **6** 155892501100600300
- 22 [42] Chung Y-C, Li Y-H and Chen C-C 2005 Pollutant Removal From Aquaculture Wastewater
23 Using the Biopolymer Chitosan at Different Molecular Weights *J. Environ. Sci. Heal. Part A*
24 **40** 1775–90
- 25 [43] Li N and Bai R 2004 Novel chitosan-cellulose hydrogel adsorbents for lead adsorption
26 *Conference Proceedings, AIChE Annual Meeting*
- 27 [44] Vachoud L and Domard A 2001 Physicochemical Properties of Physical Chitin Hydrogels:
28 Modeling and Relation with the Mechanical Properties *Biomacromolecules* **2** 1294–300
- 29 [45] Roy J C, Salaün F, Giraud S, Ferri A, Chen G and Guan J 2017 Solubility of Chitin: Solvents,
30 Solution Behaviors and Their Related Mechanisms *Solubility of Polysaccharides (InTech)*
- 31 [46] Sorlier P, Denuzière A, Christophe Viton A and Domard A 2001 Relation between the Degree
32 of Acetylation and the Electrostatic Properties of Chitin and Chitosan
- 33 [47] Guibal E 2004 Interactions of metal ions with chitosan-based sorbents: a review *Sep. Purif.*
34 *Technol.* **38** 43–74
- 35
- 36 [48] Guibal E, McCarrick P and Tobin J M 2003 Comparison of the Sorption of Anionic Dyes on

- 1 Activated Carbon and Chitosan Derivatives from Dilute Solutions *Sep. Sci. Technol.* **38** 3049–
2 73
- 3 [49] Chattopadhyay D P and Inamdar M S 2010 Aqueous behaviour of chitosan *Int. J. Polym. Sci.*
4 **2010**
- 5 [50] Iqbal J, Wattoo F H, Wattoo M H S, Malik R, Tirmizi S A, Imran M and Ghangro A B 2011
6 Adsorption of acid yellow dye on flakes of chitosan prepared from fishery wastes *Arab. J.*
7 *Chem.* **4** 389–95
- 8 [51] Chattopadhyay D P and Inamdar M S 2010 Aqueous behaviour of chitosan *Int. J. Polym. Sci.*
9 **2010**
- 10 [52] Zahrim A Y and Hilal N 2013 Treatment of highly concentrated dye solution by
11 coagulation/flocculation–sand filtration and nanofiltration *Water Resour. Ind.* **3** 23–34
- 12 [53] Bernardi F, Zadinelo I V, Alves H J, Meurer F and dos Santos L D 2018 Chitins and chitosans
13 for the removal of total ammonia of aquaculture effluents *Aquaculture* **483** 203–12
- 14 [54] Masheane M L, Nthunya L N, Malinga S P, Nxumalo E N and Mhlanga S D 2017 Chitosan-
15 based nanocomposites for de-nitrification of water *Phys. Chem. Earth, Parts A/B/C* **100** 212–
16 24
- 17 [55] Pilling M J and Seakins P W 1995 *Reaction kinetics* (Oxford University Press)
- 18 [56] Crini G and Badot P-M 2008 Application of chitosan, a natural aminopolysaccharide, for dye
19 removal from aqueous solutions by adsorption processes using batch studies: A review of
20 recent literature *Prog. Polym. Sci.* **33** 399–447
- 21 [57] Qiqi Y, Qiang H and Ibrahim H T 2012 Review on moving bed biofilm processes *Pakistan J.*
22 *Nutr.* **11** 706–13

23

24 **Acknowledgment**

25 Authors wishing to acknowledge Universiti Malaysia Sabah for funding this work (SDK 0044 –
26 2018).

27

28